

Chiral C_1 - and C_2 -Symmetrical 2,2''-Bis(1-aminoethyl)-1,1''-biferrocenes: Synthesis, Structure, and Redox Chemistry

Maurus Spescha, Noel W. Duffy, Brian H. Robinson,* and Jim Simpson*

Department of Chemistry, University of Otago, P.O. Box 56, Dunedin, New Zealand

Received July 11, 1994[⊗]

Stereospecific oxidative coupling of lithiated (*S*)-1-(dimethylamino)ethylferrocene has been used to give (*S,S*)-(*R,R*)-2,2''-bis[1-(dimethylamino)ethyl]-1,1''-biferrocene (**4**); the salt **4**·2HCl has also been characterized. Other symmetrical C_2 (*S,S*)-(*R,R*)-2,2''-bis((dialkylamino)ethyl)-1,1''-biferrocenes (alkyl = Et, morpholino) were obtained from the dimethylamino compound via acetylation followed by amination. The structure of the diethylamino representative is reported and its absolute configuration confirmed: $a = 11.700(2)$ Å, $b = 11.700(2)$ Å, $c = 17.738(4)$ Å, trigonal, $P3_2$, $Z = 3$, $R_1 = 0.0248$ (2423 reflections, $I > 2\sigma(I)$). Methylation of **4** followed by intramolecular cyclization gave the chiral cis-fused (*S,S*)-(*R,R*)-2,5''-(3,3-dimethyl-3-azoniapentane-2,4-diyl)biferrocene iodide in 95% yield and 100% diastereomeric purity. Nucleophilic attack on the azoniapropene ring unexpectedly gave the C_1 -asymmetrical 2-[1-(dialkylamino)ethyl]-2''-[1-(dimethylamino)ethyl]-1,1''-biferrocenes (alkyl = Et, morpholino, C_6H_5NH) in good yield. Electrochemical data show that the two ferrocene redox centers are weakly coupled and the redox series $[+1,+1] \leftrightarrow [1+,0] \leftrightarrow [0,0]$ is identified, but the biferrocenyl electrochemical response is modified by amine oxidation and an ECEE hydrogen abstraction mechanism when a NMe_2 substituent is present.

Introduction

Recently, a new class of Pt^{II} cytotoxic complexes incorporating a cycloplatinated ferrocenylamine as the ligand has been identified^{1,2} and its toxicity studied.³ These cycloplatinated derivatives have elements of both planar and central chirality, and included in this group are complexes with two Pt^{II} moieties per ligand in which new elements of stereochemistry are induced during cycloplatinated. Because the stereochemistry of any antiproliferative drug is likely to influence the cytotoxic action, we were interested in extending the range of ferrocenylamines with elements of chirality which could be easily obtained by stereospecific syntheses. Recent work⁴ has shown that multinuclear platinum–amine complexes may have significant antitumor activity toward *cis*-platinum-resistant cancer cells,⁵ and as an adjunct to designing ligands with a defined configuration, we required a ferrocenylamine ligand with chelating capability for at least two Pt^{II} coordination spheres. Finally, a disadvantage of the cycloplatinated complexes for drug delivery is their poor solubility in water, and we wanted a synthetic strategy which would allow the incorporation of hydrophilic substituents on the ferrocene moiety.

Chiral biferrocenylamine ligands were chosen as the target molecules, as they could satisfy all requirements. Furthermore, complexes with these ligands will form mixed-valence complexes which can give an appreciation of the parameters that affect electron-transfer rates in various electron transport chains,⁶ as well as have the potential to be radiation sensitizing agents.⁷ Two types of chiral biferrocene ligands with either a N,N (**1**) or P,P (**2**) donor set have been reported.^{8–10} These were prepared by *ortho* lithiation of the appropriate ferrocene derivative followed by oxidative coupling. By this method, Schloegl¹⁰ obtained (*R,R*)-(*R,S*)-2,2''-bis[1-(dimethylamino)ethyl]-1,1''-biferrocene, this stereoisomer resulting from heterocoupling between the major and minor components of the *ortho* lithiation. However, this stereochemistry does not orient the nitrogen lone pairs correctly for chelation; for this purpose the (*S,S*)-(*R,R*) configuration is appropriate. Also, of particular interest to our cytotoxic drug project were C_2 -biferrocenylamine ligands which have the capability of *trans*, as well as *cis*, chelation (**3**) to a Pt^{II} moiety (the configuration in a Pt^{II} –phosphine complex⁸). This paper describes synthetic routes to, and structures of, chiral C_1 - and C_2 -symmetrical 2,2''-bis(1-aminoethyl)-1,1''-biferrocenes and a new chiral cis-fused (azoniapentenediyl)biferrocene

[⊗] Abstract published in *Advance ACS Abstracts*, October 15, 1994.

(1) Ranatunge-Bandarage, P. R. R.; Robinson, B. H.; Simpson, J. *Organometallics* **1994**, *13*, 500.

(2) Ranatunge-Bandarage, P. R. R.; Duffy, N. W.; Johnson, S. M.; Robinson, B. H.; Simpson, J. *Organometallics* **1994**, *13*, 511.

(3) Mason, R.; McGrouther, K. G.; Ranatunge-Bandarage, P. R. R.; Robinson, B. H.; Simpson, J. *Toxicol. Appl. Pharmacol.*, submitted for publication.

(4) Qu, Y.; Farrell, N. P. *J. Am. Chem. Soc.* **1991**, *113*, 4851.

(5) (a) Farrell, N. P.; De Almeida, S. G.; Skov, K. A. *J. Am. Chem. Soc.* **1988**, *110*, 5018. (b) Kraker, A.; Elliott, W.; van de Houten, B.; Farrell, N. P.; Hoeschele, J.; Roberts, J. *J. Inorg. Biochem.* **1989**, *36*, 160.

(6) Brown, D. B., Ed. *Mixed Valence Compounds*; Reidel: Dordrecht, the Netherlands, 1980.

(7) (a) Joy, A. M.; Goodgame, D. M. L.; Stratford, I. J. *Int. J. Radiation Oncol. Biol. Phys.* **1989**, *16*, 1053. (b) Wenzel, M.; Wu, Y. *Appl. Radiat. Isot.* **1989**, *39*, 1237.

(8) Sawamura, M.; Yamauchi, A.; Takegawa, T.; Ito, Y. *J. Chem. Soc., Chem. Commun.* **1991**, 874.

(9) Sawamura, M.; Hamashima, H.; Ito, Y. *Tetrahedron: Asymmetry* **1991**, *2*, 593.

(10) Krajncik, P.; Kratky, C.; Schloegl, K.; Wildhalm, M. *Monatsh. Chem.* **1990**, *121*, 945.

temperature. After separation of the organic phase the aqueous phase was extracted with dichloromethane, the combined organic phases were dried over potassium carbonate, and the solvent was removed under reduced pressure. The resulting solid was extracted with hexane (2×) and the hexane stripped to give **7** (101 mg, 60%). Crystallization from hexane at -30 °C resulted in crystals suitable for X-ray diffraction. Mp: 102 °C. $[\alpha_D]^{RT} = 824^\circ$ ($c = 1.35$, ethyl acetate). Anal. Calcd for C₃₂H₁₄Fe₂N₂: C, 67.65; H, 7.75; N, 4.93. Found: C, 67.29; H, 7.90; N, 4.48. ¹H NMR (CDCl₃): δ 4.47 (m, 2H), 4.25 (s, 10H, C₅H₅), 4.21 (m, 4H), 3.85 (q, $J = 6.9$ Hz, 2H, CHCH₃), 2.16 (m, 8H, NCH₂CH₃); 1.37 (d, $J = 6.9$ Hz, 6H, CHCH₃), 0.71 (t, $J = 7.1$ Hz, 12H, NCH₂CH₃). ¹³C NMR (CDCl₃): δ 91.9, 86.5 (C1/C2); 71.7, 67.6, 65.6 (C3/C4/C5), 69.7 (C₅H₅), 50.9 (CHCH₃), 42.8 (NCH₂CH₃), 16.0, 13.9 (CHCH₃ and NCH₂CH₃).

Preparation of 2,2'-Bis[1-(morpholino)ethyl]-1,1'-biferrocene (8). A solution of **6** (prepared as for **7**) (150 mg, 0.293 mmol) in 6 mL of morpholine and 30 mL of methanol was heated to reflux for 3 h. After the mixture was cooled to room temperature, the solvents were removed under reduced pressure and most of the morpholine was removed under high vacuum. The resulting solid was extracted with ethyl acetate (2×). The crude product was purified by chromatography on silica gel (ethyl acetate) to give **8** as the hemihydrate, in 71% yield. R_f : 0.16. Mp 66 °C. $[\alpha_D]^{RT} = 514^\circ$ ($c = 1.18$, ethyl acetate). Anal. Calcd for C₃₂H₄₂Fe₂N₂O_{2.5}: C, 63.43; H, 6.83; N, 4.63. Found: C, 63.21; H, 6.55; N, 4.51. ¹H NMR: δ 4.66 (m, 2H), 4.24 (s, 10H, C₅H₅), 4.20 (m, 4H), 3.93 (q, $J = 6.9$ Hz, 2H, CHCH₃), 3.50 (m, 8H, OCH₂), 2.31 (m, 8H, NCH₂), 1.49 (d, $J = 6.9$ Hz, 6H, CHCH₃). ¹³C NMR: δ 89.1, 85.6 (C1/C2); 70.3, 67.5, 65.8 (C3/C4/C5), 69.8 (C₅H₅), 67.1 (CH₂OCH₂), 56.2 (CHCH₃), 48.6 (CH₂NCH₂), 14.7 (CHCH₃).

(S,S)-(R,R)-2,5'-(3,3-Dimethyl-3-azoniapentane-2,4-diyl)-biferrocene Iodide (9). Methyl iodide (2.7 mL, 43.3 mmol) was added to a solution of **4** (1.06 g, 2.07 mmol) in acetone (110 mL) at 0 °C. After it was stirred at this temperature for 30 min, the mixture was warmed to room temperature and stirred for a further 5 min. The solvents were removed under reduced pressure; the residue was dissolved in dichloromethane (200 mL), and this solution was stirred at ambient temperature for 24 h. The crude product obtained on evaporation was recrystallized from dichloromethane (200 mL) to give **9** as the hydrate, obtained in 95% yield as a single diastereoisomer. A small impurity with a singlet at 3.65 ppm in the ¹H NMR spectra was not removed even after several recrystallizations. Mp: 90 °C dec. $[\alpha_D]^{RT} = 663^\circ$ ($c = 0.875$, dichloromethane). Anal. Calcd for C₂₆H₃₀Fe₂IN·H₂O: C, 50.93; H, 5.26; N, 2.28. Found: C, 50.88; H, 5.18; N, 2.50. FAB-MS: 468 (M⁺). ¹H NMR: δ 4.55 (m, 4H), 4.33 (t, $J = 2.6$ Hz, 2H), 4.06 (s, 10H, C₅H₅), 4.06 (q, $J = 4.8$ Hz, 2H, CHCH₃), 2.99 (s, 6 H, NCH₃), 1.90 (d, $J = 4.8$ Hz, 6H, CHCH₃). ¹³C NMR: δ 85.4, 79.9, (C1/C2), 70.8 (C₅H₅), 69.9, 69.8, 68.8, 68.6, (C3/C4/C5/CHCH₃), 44.0 (NCH₃), 14.7 (CHCH₃).

Preparation of 2-[1-(Diethylamino)ethyl]-2'-[1-(dimethylamino)ethyl]-1,1'-biferrocene (10). A solution of **9** (50 mg, 0.084 mmol) in diethylamine, acetonitrile, and triethylamine (5 mL of each) was heated at reflux temperature for 7 h. The solvents were removed under reduced pressure, the residue was redissolved in toluene, and the solvent was removed. The crude product was purified by chromatography on silica gel (ethanol/ethyl acetate/triethylamine 100/19/1). Solvents from the bands eluting between R_f 0.48 and 0.22 were removed under reduced pressure; the residue was dissolved in dichloromethane (10 mL) and 10 mL of a saturated potassium carbonate solution was added. The resulting mixture was vigorously stirred for 1 h at room temperature. After separation of the organic phase the aqueous phase was extracted with dichloromethane and the combined organic phases dried over potassium carbonate; removal of the solvent gave **10** as the hemihydrate (28.5 mg, 62%). Mp: 95 °C. $[\alpha_D]^{RT} = 821^\circ$ ($c = 1.10$, ethyl acetate). Anal. Calcd for C₃₀H₄₀Fe₂N₂·0.5H₂O: C, 65.59; H, 7.52; N, 5.10. Found: C, 65.30;

H, 7.24; N, 5.03. ¹H NMR: δ 4.52 (m, 1H), 4.48 (m, 1H), 4.29 (s, 10H, C₅H₅), 4.29 (m, 2H), 4.24 (m, 1H), 4.20 (m, 1H), 3.90–3.95 (q, $J = 7$ Hz, 1H, CHCH₃), 2.16 (m, 4H, NCH₂CH₃), 1.82–1.87 (s, 6H, NCH₃), 1.44 (d, $J = 7$ Hz, 3H, CHCH₃), 1.43 (d, $J = 6$ Hz, $J = 6.9$ Hz, 3H, CHCH₃), 0.68 (t, $J = 7.1$ Hz, 6H, NCH₂CH₃), 0.74 (t, $J = 7.1$ Hz, 3H). ¹³C NMR: δ 91.2, 89.8, 86.1, 85.6, (C1/C1''/C2/C2''), 71.4, 70.9, 67.6, 67.2, 65.9, 65.86 (C3/C3''/C4/C4''/C5/C5''), 69.8 (C₅H₅), 55.7, 51.4 (CHCH₃), 42.7, 40.8 (NCH₂CH₃, NCH₃), 15.6, 15.0, 13.8 (NCH₂CH₃).

Preparation of 2-[1-(Dimethylamino)ethyl]-2'-[1-(morpholino)ethyl]-1,1'-biferrocene (11). A solution of **9** (96 mg, 0.161 mmol) in morpholine (10 mL) was heated at reflux temperature for 3 h. After the mixture was cooled to room temperature, liquids were removed under reduced pressure. This crude product was purified by chromatography on silica gel (ethanol/ethyl acetate/triethylamine 100/19/1). From the first separation all fractions which had the products with R_f 0.45 and 0.15 were taken (they eluted together with some impurities); from a second column separation the solvent in the bands between R_f 0.45 and 0.15 was removed under reduced pressure, the residue was dissolved in dichloromethane (10 mL), and saturated potassium carbonate solution (10 mL) was added. The resulting mixture was vigorously stirred for 1 h at room temperature, and workup as for **10** gave **11** as a hydrate (71.4 mg, 76%). Mp: 56 °C. $[\alpha_D]^{RT} = 678^\circ$ ($c = 0.895$, ethyl acetate). Anal. Calcd for C₃₀H₃₈Fe₂N₂O·1.5H₂O: C, 61.98; H, 7.11; N, 4.82. Found: C, 61.87; H, 6.64; N, 4.97. ¹H NMR (CDCl₃): δ 4.46 (m, 2H), 4.28 (m, 2H), 4.27 (s, 5H), 4.25 (s, 5H), 4.18 (m, 2H), 3.86 (q, $J = 6$ Hz, 1H), 3.68 (q, $J = 6$ Hz, 1H), 3.39 (m, 4H), 2.17 (m, 4H), 1.80 (s, 6H), 1.45 (d, 3H), 1.44 (d, 3H). ¹³C NMR: δ 89.7, 85.9, 85.6 (C1/C1''/C2/C2''), 70.8, 70.4, 67.2, 67.1, 66.2, 66.1 (C3/C3''/C4/C4''/C5/C5''), 69.9 (C₅H₅), 67.3 (OCH₂), 56.2, 55.9 (CHCH₃), 48.7 (NCH₂), 40.4 (NCH₃), 15.2, 14.3 (CHCH₃).

Preparation of 2-[1-(Dimethylamino)ethyl]-2'-[1-(phenylamino)ethyl]-1,1'-biferrocene (12). A solution of **9** (50 mg, 0.084 mmol) and aniline (0.5 mL, 5.25 mmol) in triethylamine (5 mL) and acetonitrile (2 mL) was heated at reflux temperature for 8 h. Purification on silica gel (ethyl acetate followed by ethanol/ethyl acetate/triethylamine 5.2/1/0.052) of the crude product obtained by removing the solvent gave **9** as the hydroiodide monohydrate in 90% yield when recrystallized from dichloromethane/hexane. Anal. Calcd for C₄₁H₃₇Fe₂N₂I: C, 54.42; H, 5.52; N, 3.96; Fe, 15.80. Found: C, 54.67; H, 5.23; N, 4.01; Fe, 15.60. The hydroiodide was dissolved in 10 mL of dichloromethane, 10 mL of saturated potassium carbonate solution was added, and the mixture was vigorously stirred for 1 h at room temperature. After separation of the organic phase, the aqueous phase was extracted with dichloromethane (2×) and the combined organic phases dried over potassium carbonate. Removal of the solvent gave **12** as the free amine. Mp: 56 °C. $[\alpha_D]^{RT} = 721^\circ$ ($c = 1.14$, ethyl acetate). Anal. Calcd for C₃₂H₃₆Fe₂N₂: C, 68.59; H, 6.48; N, 5.00. Found: C, 68.21; H, 6.57; N, 5.17. ¹H NMR: δ 7.04 (m, 2H, Ph), 6.62 (m, 1H, Ph), 6.41 (m, 2H, Ph), 4.41–4.24 (m, 5H), 4.30 (s, 5H, C₅H₅), 4.25 (s, 5H, C₅H₅), 4.19–4.05 (m, 2H), 3.59 (q, $J = 7.0$ Hz, 1H, CHCH₃), 1.84 (s, 6H, NCH₃), 1.49 (d, $J = 6.3$ Hz, 3H, CHCH₃), 1.21 (d, $J = 7.0$ Hz, 3H, CHCH₃). ¹³C NMR: δ 147.9, 128.8, 117.8, 116.0 (Ph), 92.5, 92.4, 85.1, 84.4 (C1/C1''/C2/C2''); 72.9, 71.8, 67.4, 67.2, 67.0 (C3/C3''/C4/C4''/C5/C5''), 70.5, 70.3 (C₅H₅), 56.4, 47.9 (CHCH₃), 41.8 (NCH₃), 20.6, 11.5 (CHCH₃).

X-ray Data Collection, Reduction, and Structure Solution for 7. Diffraction data were collected on an orange block-shaped crystal of **7** with a Nicolet R3M diffractometer at 185(5) K, using graphite-monochromated Mo K α radiation. The data were corrected for Lorentz and polarization effects,

Table 1. Crystal Data, Data Collection, and Refinement of Compound 7

empirical formula	C ₃₂ H ₄₄ N ₂ Fe ₂
mol wt	568.39
cryst syst	trigonal
space group ^a	P3 ₂ (No. 145)
a/Å	11.700(2)
b/Å	11.700(2)
c/Å	17.738(4)
α/deg	90
β/deg	90
γ/deg	120
V/Å ³	2102.8(7)
D _c /g cm ⁻³	1.347
Z	3
cryst size/mm	0.85 × 0.44 × 0.42
μ(Mo Kα)/mm ⁻¹	1.058
F(000)	906
diffractometer	Nicolet R3M
temp/K	183 ± 5
radiation	Mo Kα (λ = 0.710 69 Å)
scan type	ω
scan speed/deg min ⁻¹	6.00
data limits/deg	4 < 2θ < 50
rfins measd	h, -k, l
cryst decay ^b /%	< 1
abs cor	empirical
transmissn	0.874 (max) 0.812 (min)
total no. of rflns ^c	2752
no. of unique data (I > 2σ(I))	2423
method of solving	direct
no. of variables	338
treatment of protons	calcd
R1(ΣΔF/ε F _o)	0.0248
wR2(Σw(F _o ² - F _c ²) ² /ΣwF _o ⁴) ^{1/2}	0.0631
weight (w)	[1/(σ ² F _o ² + (0.0444P) ²) + 1.209P]; P = (Max (F _o ² , 0) + 2F _c ²)/3
goodness of fit on F ²	0.898
residual density e Å ⁻³	0.296, -0.376

^a Reference 13. ^b Standard reflections (4, -3, -4), (402), (3, -1, 5) measured after every 100 reflections. ^c Lorentz and polarization corrections and empirical absorption corrections were applied using the SHELXTL system.¹²

and empirical absorption corrections were applied using SHELXTL.¹² Analysis of systematic absences in the data was consistent with the trigonal space groups P3₁ and P3₂,¹³ and the choice of the latter alternative was vindicated by the success of the subsequent solution and refinement. Details of the crystal data collection are summarized in Table 1.

The structure was solved using SHELXS-86¹² with the resulting Fourier map revealing the location of all non-hydrogen atoms. Weighted full-matrix refinement of 7 on F² was performed with SHELXL-93.¹² Hydrogen atoms were included in calculated positions. A difference Fourier following the location of all non-hydrogen atoms revealed a second possible location for the methyl carbon atom C(32) of the ethyl residue on N(2). The disorder was resolved by refining the two atom positions, with occupancy factors tied to sum to unity. The occupancy factors converged at 0.60(1) for C(32) and 0.40(1) for C(32A) and the related H atoms. Refinement of the structure converged with R1 = 0.0248 for 2423 reflections with F_o > 4σ(F_o) and wR2 = 0.0631[8] for all 2559 data. Calculation of the Flack absolute structure parameter¹⁴ gave 0.011(17) in the final cycle, confirming that the chosen coordinates represented the correct absolute configuration of the chiral molecule. A final difference Fourier map was essentially flat with the highest peak at 0.29 e Å⁻³. Final positional and thermal

Table 2. Atomic Coordinates (×10⁴) and Equivalent Isotropic Displacement Parameters (Å² × 10⁻¹) for Compound 7^a

	x	y	z	U(eq)
Fe(1)	151.3(5)	8065.0(5)	7065.8(3)	0.02149(13)
C(1)	-1766(3)	7125(3)	6667(2)	0.0178(7)
C(2)	-1698(4)	6624(4)	7392(2)	0.0200(7)
C(3)	-1163(4)	7689(4)	7917(2)	0.0231(8)
C(4)	-906(4)	8852(4)	7520(2)	0.0243(8)
C(5)	-1270(3)	8519(3)	6747(2)	0.0200(7)
C(6)	1286(4)	7584(4)	6402(2)	0.0328(9)
C(7)	1704(4)	8937(4)	6334(3)	0.0375(10)
C(8)	2091(4)	9530(4)	7056(3)	0.0422(11)
C(9)	1902(4)	8523(5)	7575(3)	0.0386(10)
C(10)	1412(4)	7340(4)	7176(2)	0.0327(9)
C(21)	-1208(4)	9441(3)	6121(2)	0.0257(8)
C(22)	-34(5)	10855(4)	6213(3)	0.0422(11)
N(1)	-2508(4)	9360(3)	6038(2)	0.0289(7)
C(23)	-2686(5)	9756(4)	5280(2)	0.0372(10)
C(24)	-2966(5)	8727(4)	4689(2)	0.0353(10)
C(25)	-2737(6)	10103(5)	6630(2)	0.0461(12)
C(26)	-4175(6)	9769(5)	6687(3)	0.0572(15)
Fe(2)	-2421.8(5)	4702.6(5)	5517.3(3)	0.02074(13)
C(11)	-2365(3)	6358(3)	5974(2)	0.0174(7)
C(12)	-1773(4)	6627(4)	5247(2)	0.0212(7)
C(13)	-2735(4)	5774(4)	4715(2)	0.0263(8)
C(14)	-3913(4)	4953(4)	5115(2)	0.0242(8)
C(15)	-3711(4)	5290(3)	5898(2)	0.0200(7)
C(16)	-1273(4)	4212(4)	6159(2)	0.0293(8)
C(17)	-882(4)	4335(4)	5392(2)	0.0315(9)
C(18)	-1998(5)	3410(4)	4964(2)	0.0351(10)
C(19)	-3074(5)	2722(4)	5467(3)	0.0360(10)
C(20)	-2630(4)	3213(4)	6207(2)	0.0306(9)
C(27)	-4743(4)	4635(4)	6519(2)	0.0236(8)
C(28)	-5714(5)	3179(4)	6353(3)	0.0416(11)
N(2)	-5515(3)	5279(3)	6695(2)	0.0311(8)
C(29)	-6063(5)	5573(6)	6032(3)	0.0575(15)
C(30)	-7467(6)	5257(7)	6122(3)	0.071(2)
C(31)	-4846(5)	6406(4)	7197(3)	0.056(2)
C(32)	-4895(8)	6186(8)	7927(4)	0.049(3)
C(32A)	-5580(10)	6602(11)	7788(4)	0.042(4)

^a U(eq) is defined as one-third of the trace of the orthogonalized U_{ij} tensor.

parameters are listed in Table 2. Tables of thermal parameters and H atom parameters and all bond lengths and angles are deposited as supplementary material (Tables S1–S4).

Results and Discussion

The synthetic strategy adopted in this work was to examine the stereochemical nuances of the oxidative coupling of (*S,S*)-2-lithio-1-[1-(dimethylamino)ethyl]ferrocene which can be prepared in 96% diastereomeric purity from enantiometrically pure (*S*)-1-[1-(dimethylamino)ethyl]ferrocene.¹¹ To prepare the desired (*S,S*)-(*R,R*) configuration for a C₂-symmetrical 2,2''-bis(1-aminoethyl)-1,1''-biferrocene, a procedure adapted from the biaryl synthesis of Lipschutz et al.¹⁵ was initially used in our work. A higher order cuprate was formed at low temperature from (*S,S*)-2-lithio-1-[1-(dimethylamino)ethyl]ferrocene, which was then oxidized by molecular oxygen to give the (*S,S*)-(*R,R*)-biferrocenylamine 4 in 30% yield (Scheme 1). Salts were prepared by adding the acid to ether solutions of 4, and the

(12) Sheldrick, G. M. *SHELXTL an Integrated System for Solving, Refining and Displaying Crystal Structures from Diffraction Data*; University of Göttingen, 1981. SHELXS-86, a Program for the Solution of Crystal Structures from Diffraction Data; University of Göttingen, 1986. SHELXL-93, FORTRAN-77 Program for the Refinement of Crystal Structures from Diffraction Data; University of Göttingen, 1993; *J. Appl. Crystallogr.*, in press.

(13) *International Tables for X-ray Crystallography*; Kynoch Press: Birmingham, U.K., 1966; Vol. 1.

(14) Flack, H. D. *Acta Crystallogr.* **1983**, *A39*, 876.

(15) Lipschutz, B. H.; Siegmann, K.; Garcia, E. *Tetrahedron* **1992**, *48*, 2579.

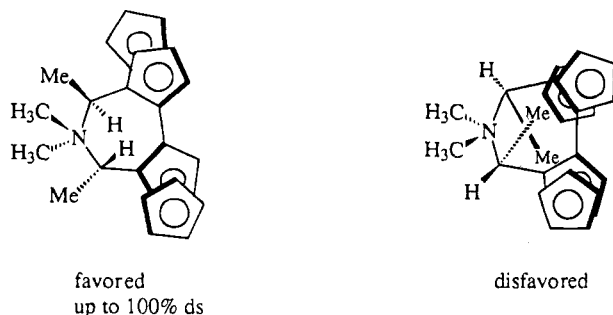


Figure 1. Possible configurations for the cyclic biferrocene **9**.

advantage that up to 40% of the starting material could be recovered (Table S5, supplementary material).

Acetylation of **4** gave the unstable diacetate **6**, which, when reacted in situ with the appropriate amine, gave **7** and **8** in good yield (Scheme 1). Hayashi¹⁷ has shown that the chirality of the amino substituent is usually maintained in this procedure, and the ¹H NMR and ¹³C NMR spectra were consistent with a C₂-symmetrical structure.

The C₂-symmetrical compound **4** was inert to butyllithium; therefore, it was not possible to introduce substituents on the cyclopentadienyl rings by the standard lithiation/electrophile route. This was unexpected, and it is a consequence of the steric congestion in this biferrocenylamine which does not allow stabilization of a lithiated intermediate by the NMe₂ lone pair. However, an alternative route to unsymmetrical biferrocenylamines was discovered, as shown in Scheme 2. Methylation of **4** led to a facile intramolecular ring closure to give the unusual chiral cis-fused (*S,S*)-(*R,R*)-(azoniapentenediyl)biferrocene **9** in 95% yield and a diastereomeric purity of 100% (determined by ¹H NMR). Its molecular structure should be the same as that of the nonchiral analogue **13** recently obtained by Hendrickson and co-workers,¹⁸ and steric considerations suggest that the chiral axis in **9** has the configuration shown in Figure 1.

In our case we were unable to isolate the trimethylammonium intermediate which undergoes intramolecular nucleophilic attack to form the azonia ring. However, in contrast to **13**, which was resistant to nucleophilic attack, we find that the azoniapropane ring in **9** is readily opened by nucleophiles. In this way the unsymmetrical biferrocenylamines **10–12** were prepared by reaction of **9** with the appropriate amine (Scheme 2). Both ¹H NMR and ¹³C NMR spectra suggest that only one single diastereoisomer is formed but the absolute configuration at the carbon atom bearing the new amino substituent and the configuration of the chiral axis between the two ferrocene moieties could not be uniquely determined. Inversion to a single (*S,R*)-(*R,R*) configuration would be expected for either a participatory S_N1 or S_N2 reaction. It is not clear why **9** is so different in reactivity toward nucleophiles compared to the nonchiral analogue **13**, but steric

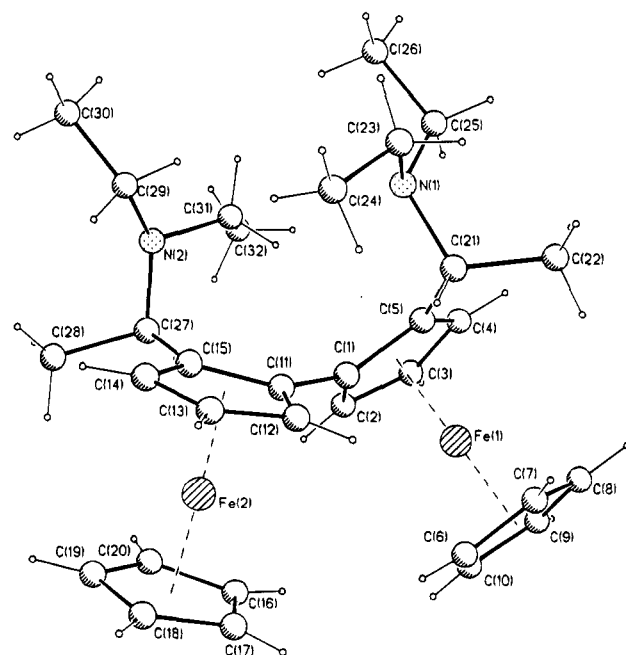


Figure 2. Molecular structure of (*S,S*)-(*R,R*)-2,2''-bis[1-(dimethylamino)ethyl]-1,1''-biferrocene (**7**) giving the atom-numbering scheme.

factors may have a role. Interactions between protons on the two unsubstituted cyclopentadienyl rings were suggested¹⁸ as the cause of the twisted structure (dihedral angle 40°) found for **13**.

Molecular Structure of 7. Confirmation of the structures and absolute configuration of the C₂-symmetrical compounds was sought from an X-ray crystal structure analysis of **7**. The structure of **7** consists of well-separated molecules in the noncentric trigonal unit cell. A perspective view of the molecule is shown in Figure 2, which also defines the crystallographic numbering scheme. Selected bond lengths and angles are presented in Table 3. The structure is that of a substituted biferrocene with the two Fe atoms linked by a fulvalene bridge carrying 2-[(diethylamino)ethyl] substituents adjacent to the C(1)–C(11) single bond. Each Fe atom also has an unsubstituted η⁵-cyclopentadiene ligand. The crystallographically determined absolute configuration (see Experimental Section) shows the configurations at C(21) and C(27) of the 2-[(diethylamino)ethyl] substituents to be *S*. The bonding parameters within the 2-[(diethylamino)ethyl] moieties are unremarkable, and the minimum energy configuration shows the chiral carbon atoms C(21) and C(27) to be roughly in the plane of the cyclopentadiene rings of the fulvalene system with the diethylamino fragments above the planes and the methyl groups C(22) and C(28) pointing toward the Fe atoms. The angles between the planes of the two sets of cyclopentadiene rings are 2.38(15)° for C(1)–C(5)/C(6)–C(10) and 1.76(22)° for C(11)–C(15)/C(16)–C(20), respectively, and the two cyclopentadiene rings of each ferrocene moiety are roughly eclipsed. The mean distances of the Fe atoms from these ring planes are 1.655(2) for both Fe(1) and Fe(2), in good agreement with the values found in ferrocene itself.²⁰

An unusual feature of this structure is that the two cyclopentadienyl rings in the fulvalene bridge are not

(17) Hyashi, T.; Mise, T.; Fukushima, M.; Kagotani, M.; Nagashima, N.; Hamada, Y.; Matsumoto, A.; Kawakami, S.; Konishi, M.; Yamamoto, K.; Kumada, M. *Bull. Chem. Soc. Jpn.* **1980**, *53*, 1138.

(18) Zhang, W.; Wilson, S. R.; Hendrickson, D. N. *Inorg. Chem.* **1989**, *28*, 4160.

(19) Harper, J.; Ranatunge-Bandarage, P. R. R.; Robinson, B. H.; Simpson, J. *Inorg. Chim. Acta*, submitted for publication.

(20) Seiler, P.; and Dunitz, J. D. *Acta Crystallogr.* **1979**, *B35*, 1068.

Table 3. Selected Bond Lengths and Angles for Compound 7

Bond Lengths (Å)			
Fe(1)–C(1)	2.068(3)	Fe(2)–C(11)	2.070(3)
Fe(1)–C(2)	2.052(4)	Fe(2)–C(12)	2.042(4)
Fe(1)–C(3)	2.039(4)	Fe(2)–C(13)	2.048(4)
Fe(1)–C(4)	2.041(4)	Fe(2)–C(14)	2.037(4)
Fe(1)–C(5)	2.061(4)	Fe(2)–C(15)	2.059(4)
Fe(1)–C(6)	2.052(4)	Fe(2)–C(16)	2.050(4)
Fe(1)–C(7)	2.043(4)	Fe(2)–C(17)	2.063(4)
Fe(1)–C(8)	2.049(4)	Fe(2)–C(18)	2.061(4)
Fe(1)–C(9)	2.050(4)	Fe(2)–C(19)	2.048(4)
Fe(1)–C(10)	2.046(4)	Fe(2)–C(20)	2.042(4)
C(1)–C(2)	1.432(5)	C(11)–C(12)	1.424(5)
C(1)–C(5)	1.439(5)	C(11)–C(15)	1.447(5)
C(1)–C(11)	1.475(5)	C(12)–C(13)	1.425(5)
C(2)–C(3)	1.425(5)	C(13)–C(14)	1.415(6)
C(3)–C(4)	1.424(5)	C(14)–C(15)	1.431(5)
C(4)–C(5)	1.431(5)	C(16)–C(17)	1.420(6)
C(6)–C(7)	1.409(6)	C(16)–C(20)	1.427(6)
C(6)–C(10)	1.425(6)	C(17)–C(18)	1.428(6)
C(7)–C(8)	1.419(7)	C(18)–C(19)	1.420(6)
C(8)–C(9)	1.423(7)	C(19)–C(20)	1.422(6)
C(9)–C(10)	1.397(6)	C(15)–C(27)	1.528(5)
C(5)–C(21)	1.524(5)	C(27)–N(2)	1.470(5)
C(21)–N(1)	1.484(5)	C(27)–C(28)	1.531(5)
C(21)–C(22)	1.542(6)	N(2)–C(29)	1.460(6)
N(1)–C(23)	1.471(5)	N(2)–C(31)	1.452(6)
N(1)–C(25)	1.471(5)	C(29)–C(30)	1.502(7)
C(23)–C(24)	1.503(6)	C(31)–C(32)	1.317(9)
C(25)–C(26)	1.528(8)	C(31)–C(32A)	1.446(8)

Bond Angles (deg)

C(2)–C(1)–C(5)	107.5(3)	C(12)–C(11)–C(15)	107.7(3)
C(2)–C(1)–C(11)	127.3(3)	C(12)–C(11)–C(1)	126.2(3)
C(5)–C(1)–C(11)	124.9(3)	C(15)–C(11)–C(1)	125.8(3)
C(3)–C(2)–C(1)	108.6(3)	C(13)–C(12)–C(11)	108.6(3)
C(4)–C(3)–C(2)	107.7(3)	C(12)–C(13)–C(14)	107.7(3)
C(3)–C(4)–C(5)	108.7(3)	C(13)–C(14)–C(15)	109.3(3)
C(4)–C(5)–C(1)	107.5(3)	C(14)–C(15)–C(11)	106.7(3)
C(4)–C(5)–C(21)	127.1(3)	C(14)–C(15)–C(27)	125.6(3)
C(1)–C(5)–C(21)	125.4(3)	C(11)–C(15)–C(27)	127.7(3)
C(7)–C(6)–C(10)	107.2(4)	C(17)–C(16)–C(20)	108.1(4)
C(6)–C(7)–C(8)	108.5(4)	C(16)–C(17)–C(18)	107.8(4)
C(7)–C(8)–C(9)	107.5(4)	C(19)–C(18)–C(17)	108.1(4)
C(10)–C(9)–C(8)	108.0(4)	C(18)–C(19)–C(20)	108.0(4)
C(9)–C(10)–C(6)	108.8(4)	C(19)–C(20)–C(16)	108.0(4)
N(1)–C(21)–C(5)	110.1(3)	N(2)–C(27)–C(28)	107.9(3)
N(1)–C(21)–C(22)	114.4(3)	N(2)–C(27)–C(15)	115.5(3)
C(5)–C(21)–C(22)	112.6(3)	C(28)–C(27)–C(15)	112.3(3)
C(25)–N(1)–C(23)	111.7(3)	C(31)–N(2)–C(29)	112.4(4)
C(25)–N(1)–C(21)	112.1(3)	C(31)–N(2)–C(27)	113.9(3)
C(23)–N(1)–C(21)	111.9(3)	C(29)–N(2)–C(27)	113.8(4)
N(1)–C(23)–C(24)	113.2(3)	N(2)–C(29)–C(30)	114.3(5)
N(1)–C(25)–C(26)	113.5(4)	C(32)–C(31)–N(2)	118.3(5)
		N(2)–C(31)–C(32A)	119.7(6)

coplanar, with an angle between the C(1)–C(5) and C(11)–C(15) ring planes of 56.77(13)°. In the majority of previously reported biferrocene structures,²¹ and a number of mixed-valence biferrocenium cations,²² the two linked ferrocene moieties are *trans* with a planar fulvalene ligand. However, none of these biferrocene systems have substituents on the fulvalene ring systems. A recent report describes the structures of neutral biferrocenes with interannular trimethylene

(21) (a) Macdonald, A. C.; and Trotter, J. *Acta Crystallogr.* **1964**, *17*, 872. (b) Kaluski, Z.; Struchov, Y. T.; Avoyan, Y. T. *Zh. Strukt. Khim.* **1964**, *5*, 743. (c) Kaluski, Z.; Struchov, Y. T. *Zh. Strukt. Khim.* **1965**, *6*, 104. (d) Kaluski, Z.; Struchov, Y. T. *Zh. Strukt. Khim.* **1966**, *7*, 283. (e) Kaluski, Z.; Struchov, Y. T. *Bull. Acad. Pol. Sci., Ser. Sci. Chim.* **1966**, *14*, 719. (f) Kaluski, Z.; Struchov, Y. T. *Bull. Acad. Pol. Sci., Ser. Sci. Chim.* **1968**, *16*, 557. (g) Kaluski, Z.; Gusev, A. I.; Struchov, Y. T. *Bull. Acad. Pol. Sci., Ser. Sci. Chim.* **1974**, *22*, 739. (h) Kaluski, Z.; Gusev, A. I.; Struchov, Y. T. *Bull. Acad. Pol. Sci., Ser. Sci. Chim.* **1976**, *24*, 631. (i) Boeyens, J. C. A.; Neuse, E. W.; Lavendis, D. C. S. *Afr. J. Chem.* **1982**, *35*, 57.

Table 4. Electrochemical Data^a

compd	A (A') ^b		B (B') ^b		C _c E _p ^c	D _c E _p ^c	G E _p ^c	log K _{diss}
	E _{1/2} ^c	ΔE _c	E _{1/2} ^c	ΔE _c				
4	0.49	90	0.79	100	0.61	0.83	0.39	5.1
7	0.53	60	0.84	100	0.60	0.79	0.33	5.3
8	0.37	80	0.63	80	0.43	0.82		4.4
9	0.65	100	0.85	70			0.35 ^d	3.4
10	0.53	70	0.83	70			0.34	5.1
11	0.49	90	0.79	100			0.39	5.1
12	0.58	80	0.86	85			0.40	4.1
14	0.57	60	0.81	92				
Fc	0.51	70						

^a Conditions: in acetone; 0.1 mol dm⁻³ TEAP on glassy-carbon electrode with SCE reference, scan rate 200 mV s⁻¹; compound 0.1 mM. Capital letters refer to redox processes defined in text; A'/B' refer to potentials after redox process G; C_c and D_c refer to cathodic component of couples A/D. ^b Italic values refer to A/B separation; values in Roman type refer to A'/B'. ^c Ferrocene under the same conditions. ^d Oxidation of I⁻.

bridges between the fulvalene and cyclopentadiene rings and the cation derived from one of them.²³ These molecules display a similar fulvalene ring twisting, which was ascribed to the steric demands of the interannular bridge systems. For 7, the presence of the bulky 2-[(diethylamino)ethyl] substituents on the cyclopentadiene rings of the fulvalene would also have significant steric consequences and are the probable cause of the ring twisting observed here.

Redox Chemistry. The anodic electrochemical responses of these biferrocenylamines were complicated by amine oxidation and can be grouped: 8 with two morpholine substituents, those compounds with at least one NR₂ function (4, 7, 10–12), and the cation 9; data are summarized in Table 4.

Compound 8. Current–voltage curves for 8, which has two identical ferrocenylamine redox centers, displayed two chemically and electrochemically reversible oxidation couples (A and B, Figure 3a) separated by 260 mV over a sweep range of 0.02–10 V s⁻¹ at Pt or GCE in acetone. E_{1/2} for the first process at 0.37 V is negative of that for the ferrocene couple under the same conditions. Multiscan responses in the range 0.0–1.0 V are superimposable, showing that both redox processes are chemically and electrochemically reversible. The *i*_{pa}/*i*_{pc} ratio is unity, and linear *i*_{pa} vs *v*^{1/2} plots are consistent with a one-electron transfer for each process.²⁴ With extension of the potential range > 1.0 V the new process E due to the oxidation of the morpholine substituent is seen at ~1.2 V on the anodic scan (the same potential as for morpholine itself) and, on the cathodic scan, the three new waves C_c, D_c (Figure 3b), and F (again, this reduction process is found in morpholine itself). Successive scans then contain these new cathodic waves and the two new waves C_a and D_a on the anodic scan, providing the cathodic scan does not reach F; if the

(22) (a) Konno, M. *Acta Crystallogr.* **1981**, *37*, C219. (b) Konno, M.; Hyodo, S.; Iijima, S. *Bull. Chem. Soc. Jpn.* **1982**, *55*, 2327. (c) Kohn, M. J.; Dong, T.-Y.; Hendrickson, D. N.; Geiby, S. J.; Rheingold, A. L. *J. Chem. Soc., Chem. Commun.* **1985**, 1095. (d) Dong, T.-Y.; Kohn, M. J.; Hendrickson, D. N.; and Pierpont, C. G. *J. Am. Chem. Soc.* **1985**, *107*, 4777. (e) Dong, T.-Y.; Hendrickson, D. N.; Iwai, K.; Kohn, M. J.; Geiby, S. J.; Rheingold, A. L.; Sano, H.; Motoyama, I.; Nakashima, S. *J. Am. Chem. Soc.* **1985**, *107*, 7996. (f) Dong, T.-Y.; Hendrickson, D. N.; Pierpont, C. G.; Moore, M. F. *J. Am. Chem. Soc.* **1986**, *108*, 963. (g) Geiby, S. J.; Rheingold, A. L.; Dong, T.-Y.; Hendrickson, D. N. *J. Organomet. Chem.* **1986**, *312*, 241. (h) Konno, M.; Sano, H. *Bull. Chem. Soc. Jpn.* **1988**, *61*, 1455.

(23) Dong, T.-Y.; Lee, T.-Y.; Wen, Y.-S.; Lee, S.-H.; Hsieh, C.-H.; Lee, G.-H.; Peng, S.-M. *J. Organomet. Chem.* **1993**, *456*, 239.

(24) Bard, A. J.; Faulkner, L. R. *Electrochemical Methods: Fundamentals and Applications*; Wiley: New York, 1980.

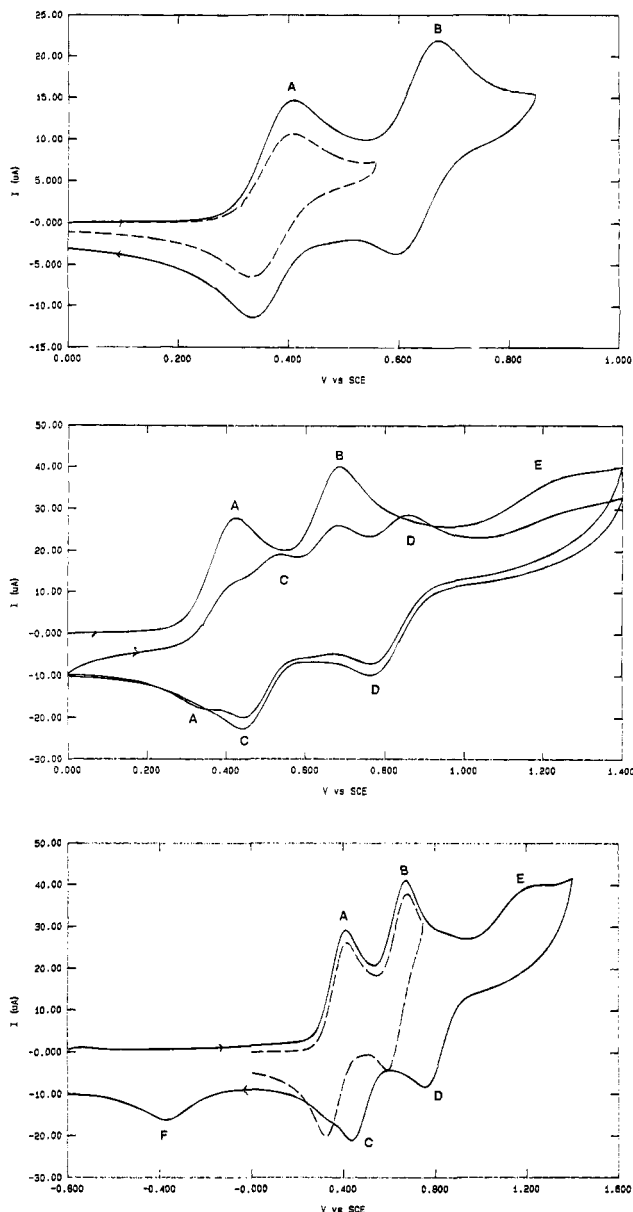
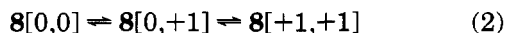


Figure 3. Cyclic voltammograms of **8** in acetone (at Pt, 0.1 TEAP; V vs SCE at 298 K): (a, top) 200 mV s^{-1} ; (b, middle) 500 mV s^{-1} , 0.0–1.4 V scan range; (c, bottom) 200 mV s^{-1} , -0.8 to -1.6 V scan range.

successive scans include **F**, then only the initial anodic components of **A** and **B** are seen (Figure 3c).

These electrochemical data are consistent with a mixed-valence compound with two weakly interacting ferrocene redox centers (eq 2). Oxidation of the mor-



pholine substituent then sets up alternative redox couples **C/D** at a potential positive to couples **A/B**. Reduction of the oxidized morpholine species occurs at **F**, and since couples **A/B** reappear, oxidation of the morpholine cannot lead to a major structural change in the biferochenylamine backbone. Extensive work has shown²⁵ that the primary electrode process for amines is the transfer of an electron from the N-donor to the electrode to form a cation radical. An aromatic system

(25) Ross, S. D.; Finkelstein, M.; Rudd, E. J. *Anodic Oxidation*. Academic Press: New York, 1975.

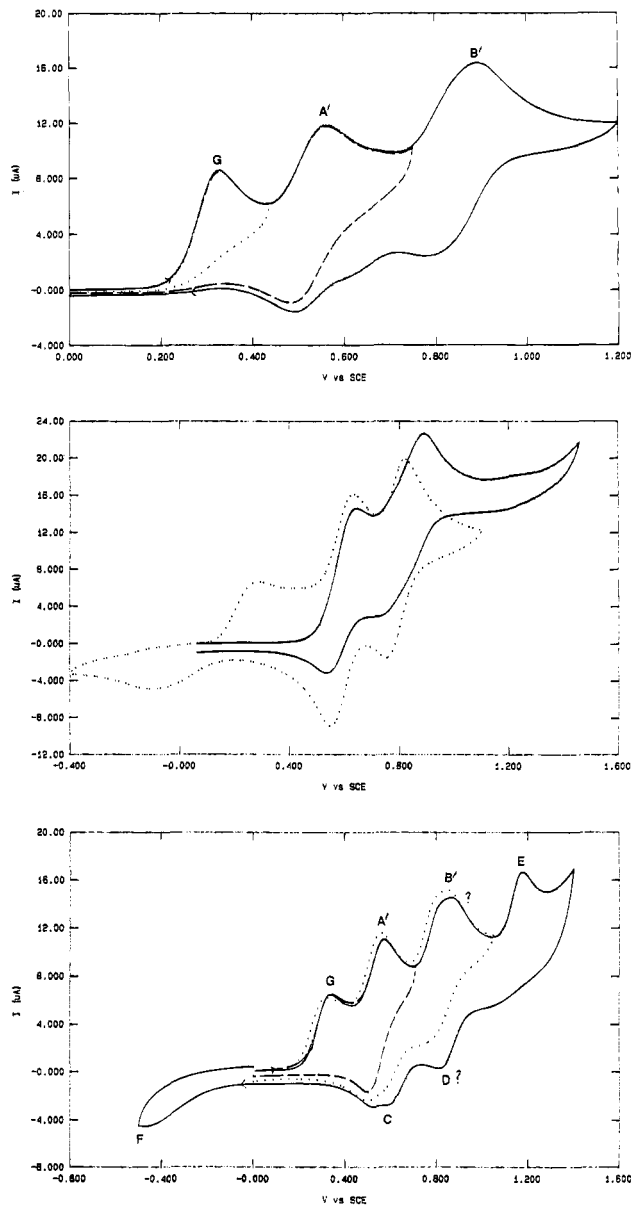
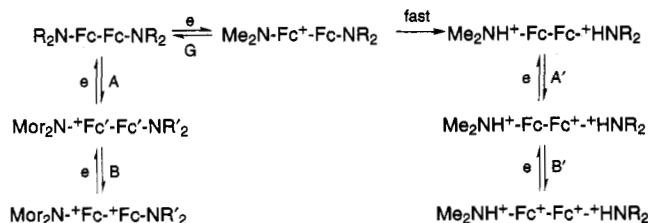


Figure 4. Cyclic voltammograms in acetone (at Pt, 0.1 M TEAP; V vs SCE): (a, top) **10** (1 mM), 100 mV s^{-1} at 298 K; (b, middle) **14** (—) and **4** (···) 200 mV s^{-1} , at 213 K; (c, bottom) **10**, 100 mV s^{-1} , extended range at 298 K.

stabilizes the cation radical, but with aliphatic amines both proton transfer and dealkylation to give an amine of lower order and an aldehyde are facilitated. The oxidative electrochemistry of morpholine is dependent on several factors, especially pH, and further work is required to elucidate the amine oxidation mechanism for **8**.

Compounds 4, 6, 7, and 10–12. Initial i - V plots for this group, which have one or two NMe_2 or NEt_2 substituents, are characterized by an additional oxidation step. The oxidation wave **G** at ~ 0.36 V, which is chemically irreversible up to 20 V s^{-1} at Pt or GCE, is followed by two chemically reversible, one-electron couples **A/B'** (Figure 4a). Irrespective of the substituent, **G** is irreversible and **A'** is chemically reversible if the scans are switched before **B'**. Electrochemical profiles are coincident over repeat scans between 0.0 and 0.9 V for scan rates < 200 mV s^{-1} , but at faster scan rates the current of **G** decreases relative to **A/B'**. The current ratio $i(\mathbf{G})/i(\mathbf{A}')$ also depends on the amine

Scheme 3

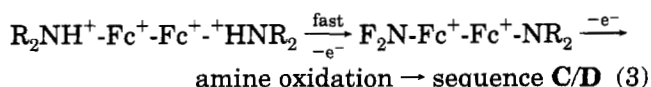


substituent, varying between ~ 0.6 for **12** and ~ 1.3 for **7** at 100 mV s^{-1} . The potential for **G** is similar to that for couple **A** in **8**, but the irreversibility of **G** and its variable current relative to **A/B'** would not be expected for a biferrocene couple. Controlled-potential electrolysis of **4** at **G** gave several products, but the major species was the salt **14**. Formation of the salt **14** simplified the responses for **4** such that only the chemically and electrochemically reversible couples **A/B'** were observed.

By comparison, electrochemical responses for the ferrocenylamine analogue [(dimethylamino)ethyl]ferrocene show a single reversible one-electron couple at $E_{1/2} = 0.49 \text{ V}$, the irreversible wave **E** at 1.19 V due to oxidation of the amine, but no feature corresponding to **G**. Therefore, while it is clear that **E** for this group of biferrocenylamines arises from the oxidation of the NR_2 substituent, process **G** is unlikely to involve amine oxidation *per se*, although it is specific to compounds with NMe_2 or NEt_2 substituents. Couples **A/B'** for this group correspond to the oxidation of the ferrocenyl moiety of the *product* of process **G**. A feasible ECEE mechanism for the NMe_2 compounds and an EE mechanism for compounds without an aliphatic alkyl substituent are given in Scheme 3 (mor = morpholino, Fc = $\text{C}_5\text{H}_3\text{CH}(\text{CH}_3)$, $R' \neq \text{Me}$ or Et).

After the first anodic oxidation to the $[0,+1]$ species at **G** the mixed-valence species rapidly abstracts a hydrogen atom from the solvent to give a salt, and it is this species which is associated with couples **A/B'** at more positive potentials of couples **A/B** as expected. The mechanism is consistent with the same electrochemical profiles for **4** and **14**, and it is similar to that invoked for tertiary amines.²⁵ The high $\text{p}K_b$ for NR_2 -substituted biferrocenylamines¹⁹ must assist this process, and it is possible that the face-to-face orientation of a (*S,S*)-(*R,R*) biferrocene configuration provides a pathway for electronic reorganization and specific hydrogen atom transfer. Hendrickson¹⁸ has proposed a similar intramolecular redistribution of charge for the oxidation of a neutral cyclic bridged amine compound analogous to **13**; in this case oxidation of the cyclic amine rather than the ferrocenyl unit is observed.

Additional cathodic features **C/D_c** are seen if the switching potential is post-**E** (Figure 4c). Since **E** is due to amine oxidation, we infer that deprotonation has occurred at **B'** (eq 3). There is evidence of another anodic process close to the potential of **B'**. The high cationic charge on the $[+1,+1]$ species would destabilize the protonated form and encourage deprotonation.



Compound 9. **9** provides an interesting comparison to the last group, as the two ferrocene redox centers are

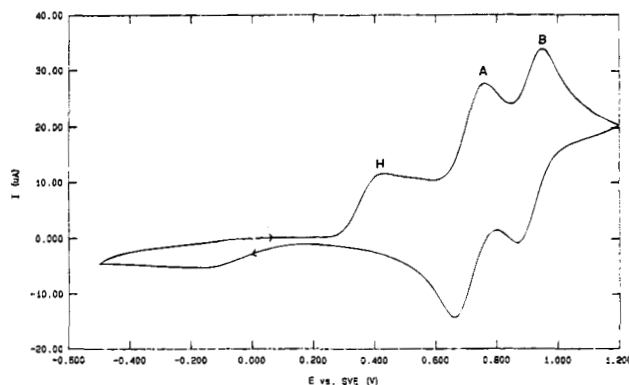
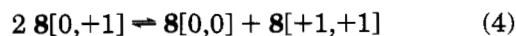


Figure 5. Cyclic voltammogram of $0.1 \text{ mM } \mathbf{9}$ (0.1 M TEAP , scan rate 100 mV s^{-1} at Pt at 298 K).

now linked by both a fulvalene and azonia bridge in a symmetrical biferrocenylamine, but there is no terminal NR_2 group. Again, the three features **A** and **B** (separated by 180 mV) and **F** (at a potential similar to that of **G**) are seen (Figure 5) on the anodic scan. An assignment of **F** to oxidation of the counterion I^- was substantiated by comparison with the electrochemistry of LiI in acetone and the increase in current function for **F** when I^- was added to the solutions of **9**; a wave attributable to the reduction of I_2 was seen at -0.20 V . In contrast to **8**, the oxidation processes associated with the ferrocene redox centers in **9** are not fully chemically reversible at slow scan rates; this irreversibility is unaffected by the switching potential and is probably caused by the liberated I_2 (no electrochemistry was recorded for **13** because of this problem¹⁸). The $E_{1/2}$ values for **9** are more positive than those for **8**, reflecting the existence of a positively charged bridge which acts as an electron-withdrawing substituent.

Despite the complications induced by the rapid hydrogen abstraction upon oxidation of the ferrocenyl unit and amine oxidation, compounds **4** and **7–12** all display class II mixed-valence behavior. Disproportionation equilibrium constants K_{diss} (e.g. eq 4) can be calculated



from the separation between **A** and **B**, or **A/B'** (Table 4), and, with the exception of that for **9**, they are similar to the value for biferrocene (1.7×10^{-6}) and are unaffected by protonation of the terminal amine group. The mixed-valence species should therefore be accessible on the synthetic time scale, but to avoid complications from competing reactions, only the redox behavior of **8** was studied in solution. Oxidation in an OTTLE cell at **A** produced a color change from yellow to red with the appearance of a broad intravalence transfer band at 1600 nm ; the very low extinction coefficient (200) suggested that complete oxidation to the $[0,+1]$ species had not occurred. A similar result was obtained with $1 \text{ mol of Ag}^{\text{I}}$ but with excess Ag^{I} ($> 4 \text{ mol}$) a purple solution was obtained with no bands $> 600 \text{ nm}$ and a broad band $\lambda_{\text{max}} 560 \text{ nm}$; it is likely that both Ag^{I} coordination and oxidation had taken place.

Conclusion

The compounds described herein provide a new series of biferrocenylamines which could be useful in several areas of research. They can be utilized as ligands for a

Pt^{II} coordination sphere and hence for the synthesis of complexes with potential biological activity. In particular, the cyclic intermediate **9** and the diacetate **6** offer a route to sugar biferrocenylamines, the sugar providing the hydrophilic group needed to confer water solubility in these systems. The unexpected facile nucleophilic attack on the cis-fused azoniapropane ring **9** opens a new route to the synthesis not only of unsymmetrical biferrocenylamines but also of unsymmetrical biferrocenes with substituents other than amines. Mixed-valence species derived from these biferrocenylamines will be used to investigate the effect of interannular bridge, chirality, and solid-state structure on intramolecular electron-transfer rates, which are known²⁶ to be dependent on a number of factors. Finally, the facile anodic oxidation of the biferrocene substituent can be

(26) (a) Dong, T.-Y.; Lin, H. M. *J. Organomet. Chem.* **1992**, *426*, 369.
(b) Webb, R. J.; Dong, T.-Y.; Pierpont, C. G.; Boone, S. R.; Chadha, R. K.; Hendrickson, D. N. *J. Am. Chem. Soc.* **1991**, *113*, 4806.

used to synthesize other biferrocene compounds and to probe long-range interactions in chiral biferrocenylamines.

Acknowledgment. We thank the Swiss Cancer Institute for a Fellowship, the Swiss Volksbank for financial support (to M.S.), and Professor W. T. Robinson, University of Canterbury, for the X-ray data collection.

Supplementary Material Available: Tables of bond distances and angles, anisotropic displacement parameters, and hydrogen coordinates and isotropic displacement parameters for **7** and a table giving product distribution, reaction conditions, and yields for the formation of the biferrocene **4** (6 pages). Ordering information is given on any current masthead page.

OM940543F